Ecological Indicators 104 (2019) 626–635

Contents lists available at ScienceDirect

Ecological Indicators

journal homepage: www.elsevier.com/locate/ecolind

Impacts of idealized land cover changes on climate extremes in Europe

Xiangping Hu, Bo Huang*, Francesco Cherubini

Industrial Ecology Programme, Department of Energy and Process Engineering, Norwegian University of Science and Technology (NTNU), Trondheim, Norway

ARTICLE INFO

Keywords:
Climate extremes
Land cover change
Deforestation
Afforestation
Maximum temperature and precipitation
Regional climate model

ABSTRACT

Extremes in climate and weather can pose significant challenges to economy, ecosystems and human health. Changes in land cover are one of the drivers for variability in frequency and magnitude of extreme climate at regional and local levels. In this study, a regional climate model (COSMO-CLM v4.8) is used to simulate effects in climate extremes from two different idealized land cover change scenarios in Europe. These two simulations involve abrupt large-scale conversion of today forestland to herbaceous vegetation (deforestation), and of today cropland to evergreen needle-leave forest (afforestation). A control simulation with today land cover distribution is used to identify differences in extreme climate. We find significant changes in extreme climate in both deforestation and afforestation simulations, with seasonal and spatial differences. Deforestation causes a warmer summer (with higher annual maximum temperature) and a colder winter (with lower annual minimum temperature). Afforestation slightly increases the average intensity of the hot extremes, although with high spatial variability (a reduction is common in several locations), and mitigates cold extremes in winter. Changes in extreme indices show that deforestation increases both the frequency and duration of hot and cold extremes, while afforestation causes a lower frequency of extreme cold climate. The two simulations show opposing results in the number of frozen days, as they increase for deforestation and decrease for afforestation. A drier climate is found after deforestation, whereas a wetter climate is observed after afforestation. In general, deforestation and afforestation increase the frequency of hot extreme climate as they reduce the return period and increase the return level. Overall, our findings show the potential critical effects that land cover changes can have on climate extremes, and the possible synergies that land management strategies and planning can have for climate change mitigation and adaptation at a regional scale.

1. Introduction

Extremes in climate and weather are a challenge for human societies and ecosystems. For example, heat waves are frequently associated with excess mortality (Pirard et al., 2005; Astrom et al., 2013; Mitchell et al., 2016; Mora et al., 2017), and average higher temperatures in winter nights favors survival of pests across the winter (Peterson et al., 2008), thereby increasing insect outbreaks with potentially large effects on the carbon cycle (Arora et al., 2016). Heat waves also increase the risk of natural disasters, such as forest fires (Seidl et al., 2014). The diffusion processes of extreme climate also impact on environmental sustainability (Aldieri and Vinci, 2018; Hájek and Stejskal, 2018). It is thus important to understand not only how these extremes are changing over time, but also their drivers and opportunities for mitigation and adaptation.

Extreme climate is an un-normal climate which occurs at a particular time and place (Hegerl et al., 2007). It is defined as the occurrence of a value of a climate or weather variable which is above or below a given threshold in the tail of the observed values of the variable (Seneviratne et al., 2012). The analysis of extreme events thus focuses on investigating the behavior of the events with very low probability (Zhang and Zwiers, 2013). The definition of extreme events in climate and weather fits well to statistical science, and it facilitates the use of classical statistical theories and the corresponding tools for detecting changes in extremes (Coles et al., 2001; Katz et al., 2002; Beirlant et al., 2006; Reiss et al., 2007; Gilleland et al., 2013; Gilleland and Katz, 2016). With these theories and tools, it is possible to analyze extreme events that are beyond the range of the datasets. For instance, based on a 30-year sample, it is possible to predict the event that only happens every 50-year or 100-year. It is also possible to calculate how rare an event is expected to occur for a given extreme value. Understanding of extreme events is a crucial objective for climate mitigation and ecosystem/society adaptation in a risk assessment framework, which requires to investigate the behaviors in the tails of the probability density function (PDF).

In order to harmonize the analysis on extreme events, several widely

* Corresponding author.
E-mail address: bo.huang@ntnu.no (B. Huang).

https://doi.org/10.1016/j.ecolind.2019.05.037
Received 31 August 2018; Received in revised form 15 March 2019; Accepted 14 May 2019
Available online 23 May 2019

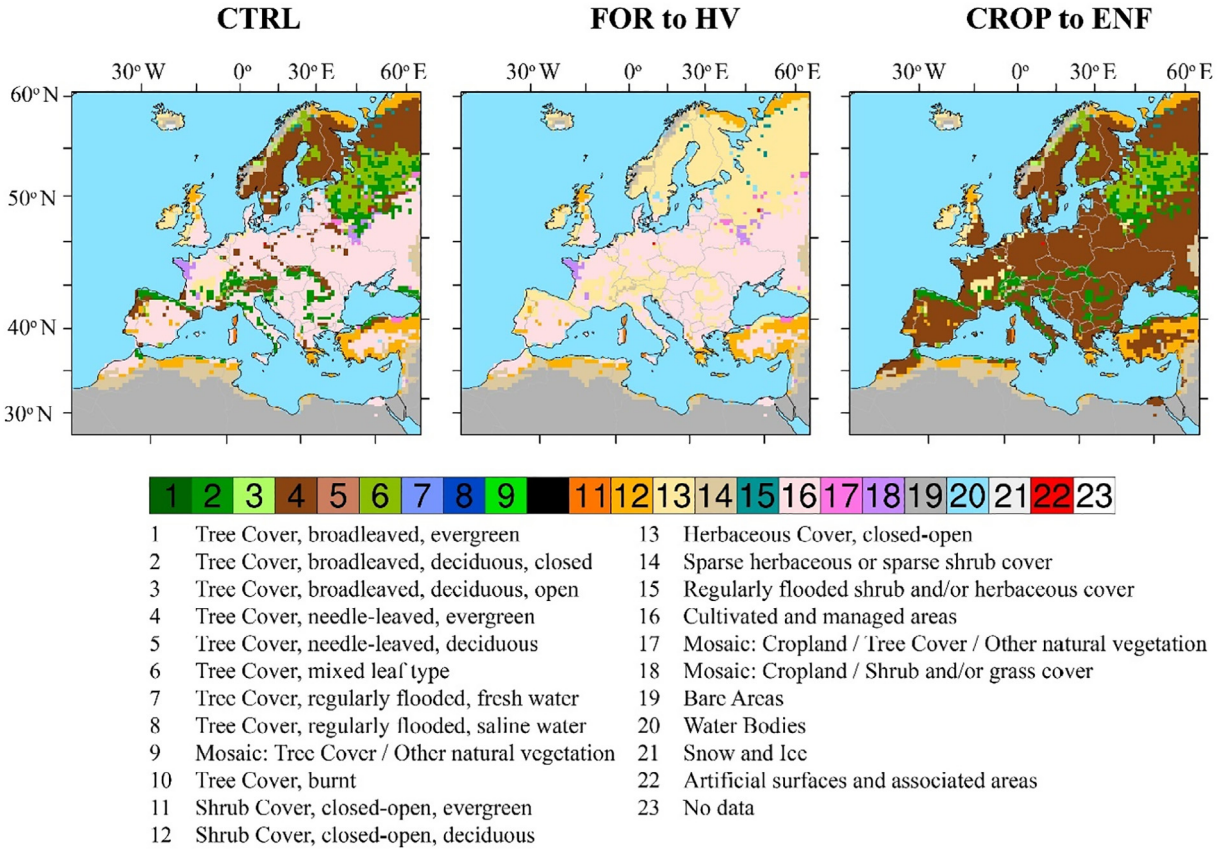

Fig. 1. Spatial distribution of the dominant land covers in the control simulation (CTRL), forest to herbaceous vegetation (FOR to HV) and cropland to evergreen needle-leaf forest (CROP to ENF), in the EURO-CORDEX domain.

used descriptive indices have been defined (Frich et al., 2002; Alexander et al., 2006; Tank et al., 2009; Zhang et al., 2011). Previous studies show that land cover changes (LCC) alter land-atmosphere processes, with changes in local temperature and precipitation (Seneviratne et al., 2010; Stefanon et al., 2014; Cherubini et al., 2016), including extremes (Davin et al., 2014; Findell et al., 2017; Lejeune et al., 2018). Land-atmosphere processes change local energy transfer and water cycle, and merge to large scale general circulation to interact to other climate systems (Findell et al., 2009). Open lands such as cropland or grassland are frequently measured to be warmer than forests during daytime in summer, although there are sometimes contrasting outcomes due to regional differences and experimental approaches (Easterling et al., 2000; Davin et al., 2014; Findell et al., 2017).

In this paper, we investigate several extreme indices including warm and cool days and nights, frozen days, warm and cold spell duration, and consecutive dry and wet days, under different idealized large-scale LCCs in Europe using a regional climate model. We apply the classical extreme value theories and tools to compare the changes in probability of extreme events in our datasets from different simulations, i.e. a control run under present land cover against simulations after land cover changes.

2. Materials and methods

2.1. Model configuration

The simulations are performed with the regional climate model Consortium of Small scale Modelling (COSMO-CLM; v4.8) (Rockel et al., 2008). COSMO-CLM is a non-hydrostatic climate model. It has been widely used in dynamical downscaling, regional climate modeling and for research on land-atmosphere interactions in Europe (Kotlarski et al., 2014; Davin et al., 2016; Cherubini et al., 2018). The model uses the split-explicit third-order Runge-Kutta time discretization on the Arakawa-C horizontal grid (Arakawa and Lamb, 1981; Wicker and Skamarock, 2002). Characteristics of the terrain is based on height coordinates with rotated geographical coordinates in the vertical level (Schär et al., 2002). Turbulent kinetic energy is used as a prognostic variable for vertical turbulent mixing parametrized according to a level 2.5 closure (Mellor and Yamada, 1982). The moist convection is described by the Tiedtke (1989) mass flux scheme, and the radiative fluxes are calculated by the δ-two stream radiative transfer scheme (Ritter and Geleyn, 1992). Biophysical exchange processes between the atmosphere, land surface, and soil are presented by the soil-vegetation-atmosphere model TERRA-ML (Schrodin and Heise, 2001). The turbulent exchange between the underlying surface and the atmosphere in TERRA-ML is modeled by a stability and roughness length-dependent surface flux (Doms and Schättler, 2002; Ament and Simmer, 2006). TERRAL-ML calculates the hydrological processes by soil moisture diffusion between 10 soil layers up to 15 m. At each grid cell, the soil texture and dominant vegetation type are taken from gridded observation. The vegetation type is classified by different parameters including plant coverage, leaf area index, roughness length, and root depth.

2.2. Simulations

In our study, one control run and two simulations with idealized LCC are performed. All simulations follow the EURO-CORDEX framework and use the same configuration as COSMO-CLM in EURO-COREX (Kotlarski et al., 2014). We use the European Centre for Medium-Range Weather Forecasts Interim reanalysis (Dee et al., 2011) to drive

COSMO-CLM between 1980 and 2010. The first simulation year is excluded from further analysis as it is a spin-up time. The simulations are integrated at 0.44° (~50 km) horizontal resolution, 40 atmospheric vertical levels, and 300 s for a time step.

We first conduct a control simulation (CTRL) with the present-day soil and vegetation cover using the global land cover database GLC2000 (GLC, 2005). This simulation is used as the baseline scenario. Then, we set up two idealized simulations based on extreme land cover changes to maximize model's response, which are called deforestation and afforestation simulations, respectively. One replaces all the forested grid cells in Europe with herbaceous vegetation (FOR to HV), and the other one replaces all the cropland grid cells with evergreen needle-leaf forest (CROP to ENF). In each changed pixel, we change the dominant land cover at each grid cell by modifying the land cover parameters. These prescribed parameters have strong seasonal difference but are constant without year-to-year variation. The change in plant cover are represented by changes in vegetation coverage, roughness length, root depth and LAI (Tölle et al., 2017). Serval studies used this method to study the interactions between LCC and climate (Tölle et al., 2014, 2017; Cherubini et al., 2018; Tölle et al., 2018). In the deforestation simulation, the land cover transition mainly occurs in eastern and northern Europe, and in the afforestation simulation the land cover transition primarily takes place in central Europe covering the middle part of the domain from east to west (Fig. 1).

2.3. Statistical indices of extremes

To quantify the impact of LCC on extreme climate in Europe, we analyze the changes of extreme climate indices between the FOR to HV, CROP to HV and the CTRL simulation. We select nine extreme climate indices for further analysis. The definition and abbreviation of the indices (Table 1) follow the standard report on climate change detection (Peterson et al., 2001). These indices have been widely used in the existing literature (Klein Tank and Können 2003; Vincent and Mekis, 2006; Zhang and Zwiers, 2013; Sheikh et al., 2015). We use the daily maximum and minimum temperature to calculate the indices of extremes involving temperature. Precipitation (PR) is selected to compute extreme indices related to wet days. We also show the changes of average annual maximum temperature (TASMAX) and average annual minimum temperature (TASMIN).

2.4. Extreme values theory

Extreme climate events can be investigated with the extreme value analysis (AghaKouchak et al., 2012; Fischer and Knutti, 2015; Gomes and Guillou, 2015). Previous studies successfully applied the statistical extremal value theory to hydrology and environmental systems in general (Naveau et al., 2005; Katz, 2013; Cheng et al., 2014), including specific applications related to climate change and risks (Coles et al., 2001; Peterson et al., 2008; AghaKouchak et al., 2012; Cooley, 2013; Findell et al., 2017).

In this paper, the extreme values theory is applied to the three simulations described above in order to investigate the changes in long-term low probability extremal events, such as the return level and return period. These two concepts are frequently used to quantify risks (Cooley, 2013). In general, the extreme events M_n can be explained as

$$M_n = \max\{X_1, X_2, \ldots X_n\} \tag{1}$$

where $\{X_i; i = 1, 2, \ldots, n\}$ is a sequence of independent random variables and identically distributed with a common statistical distribution. The Extremal Types theorem states that suppose there exist the normalizing constants, $a_n > 0$ and b_n, such that

$$\mathrm{P}\{(M_n - b_n)/a_n \le x\} \to G(x) \quad \text{as } n \to \infty \tag{2}$$

where P denotes the probability, and then the cumulative distribution function G is a generalized extreme value (GEV) distribution (Coles et al., 2001),

$$G(x; \mu, \sigma, \xi) = \exp\left\{-\left[1 + \xi\left(\frac{x-\mu}{\sigma}\right)\right]^{-1/\xi}\right\} \tag{3}$$

with the condition $1 + \xi(x-\mu)/\sigma > 0$, the location parameter $-\infty < \mu < \infty$, the scale parameter $\sigma > 0$ and shape parameter $-\infty < \xi < \infty$. Using this notation, the GEV distribution can have three different types, a Fréchet type ($\xi > 0$ with a heavy tail), a Weibull type ($\xi < 0$ with a bounded tail) and a Gumbel type (the limit as $\xi \to 0$ with a light tail) (Coles et al., 2001; Katz, 2013). Own to the unification of the three types of extreme value distribution to a single GEV distribution, we can use the data to determine the best appropriate type of tail behavior through the inference on the shape parameter ξ.

The GEV distribution has theoretical foundation for modeling the block maxima of data, such as annual maxima, and the quantiles of the GEV distribution are commonly interpreted as return levels (Coles et al., 2001; Cooley, 2013; Gilleland et al., 2013; Gilleland and Katz, 2016). Therefore, we analyze the quantiles using annual maximum series from our simulations. By inverting Eq. (2), we can get the extreme quantiles of the annual maximum distribution

$$x_p = \begin{cases} \mu - \frac{\sigma}{\xi}[1 - [-\log(1-p)]^{-\xi}], & \xi \neq 0 \\ \mu - \sigma\log[-\log(1-p)], & \xi = 0 \end{cases} \tag{4}$$

with $G(x_p) = 1 - p$, and x_p is called the return level in common terminology, and correspondingly, $1/p$ is called the return period. We assume that both the return level and return period are stationarity, where the return level is constant every year, the return level x_p is exceeded by the annual maximum with probability p in any particular year. The return period inverts to the probability p (Coles et al., 2001; Cooley, 2013).

3. Results

3.1. Changes in the indices of extremes

To understand the effects on extreme climate from land cover changes in CCLM, we assess nine commonly used extreme indices

Table 1
Definition and abbreviation of the extreme indices considered in this study (Zhang and Zwiers 2013).

Indices	Indicator name	Definition	Units
TX90%	warm days	number of days with daily max temperature above the 90th percentile per year	days
TN90%	warm nights	number of days with daily min temperature above the 90th percentile per year	days
TX10%	cool days	number of days with daily max temperature below the 10th percentile per year	days
TN10%	cool nights	number of days with daily min temperature below the 10th percentile per year	days
FD	Frost days	number of days with daily minimum temperature below 0 °C	days
WSDI	warm spell duration indicator	number of 6 consecutive days above daily max temperature above the 90th percentile per year/season	
CSDI	cold spell duration indicator	number of 6 consecutive days with daily min temperature below the 10th percentile per year/season	
R95%	very wet days	number of days with precipitation above 95th percentile per year	days
R99%	extremely wet days	number of days with precipitation above 99th percentile per year	days

Table 2
Changes of the extreme indices in the deforestation and afforestation simulations compared to the control simulation.

	FOR to HV		CROP to ENF	
	Regional	Local	Regional	Local
TX90%	1.1	4.1	4.6	6.2
TN90%	1.2	6.2	1.0	−2.2
TX10%	3.0	9.9	−8.9	−0.
TN10%	4.6	9.7	−8.8	−0.2
FD	2.0	6.1	−1.3	−3.2
WSDI	0.3	0.9	0.9	1.2
CSDI	0.9	1.7	−0.1	−2.1
R95%	−1.4	−4.8	0.6	3.0
R99%	0.1	−0.6	0.6	1.2

(Table 2). On the regional and local scale (i.e. grids affected by land use change only), the TX90%, TN90%, TX10%, TN10% and FD show a positive response to deforestation (Table 2). The effects on the extremes are more relevant when the indices are averaged in the grid cells with LCC (i.e. local scale). This means that forest clearance exacerbates temperature extremes in both winter and summer. Deforestation is also found to decrease precipitation extremes, as the climate becomes drier because less water is transpired to the atmosphere. This can also lead to a reduction of cloud cover, with land surface absorbing more solar radiation thereby further changing the surface extreme temperatures. A similar finding has been reported in previous studies (Tölle et al., 2017).

The afforestation simulation (CROP to ENF) shows a different pattern in the climate response than deforestation. On the regional scale, there is a slight increase of TX90% and TN90%. A more noticeable change is found in TX10% and TN10%. Afforestation also reduces the number of FD. The corresponding results on the local scale generally follow the same pattern but are more significant, except for the number of warm nights that turns to negative. This is due to the presence of needle-leaf trees which reduce the surface albedo, and the net radiation on the surface increases (Cherubini et al., 2018; Hu et al., 2018). This finding is in line with results from other studies (Bala et al., 2007; Davin and de Noblet-Ducoudre, 2010; Wang et al., 2014; Cherubini et al., 2018).

Compared to the CTRL simulation, in the deforestation simulation the regional mean of WSDI increases of 0.28 day, and of 0.94 day on the local scale. The change of CSDI is more significant than the WSDI, with 0.89 day and 1.70 day, at regional and local scale, respectively. However, afforestation raises the WSDI, but reduces CSDI. Deforestation leads to a higher occurrence frequency of TX90%, up to six days, but with large variability, and the number of TX90%, up to 10 days (Fig. 2). Afforestation increases the occurrence of TX90% with up to 5 days, but significantly reduces the number of days for TN10% (8.8 days on regional scale).

Compared to the CTRL run, deforestation decrease R95% and R99% while afforestation increases the days for both R95% and R99%. On the local scale, the reduction of R95% and R99% indicates that a lower frequency of heavy rainfall occurs when the forest land is replaced by HV. Increases in R95% and R99% in CROP to ENF simulation shows that afforestation leads to a higher frequency of heavy rainfall. Similar

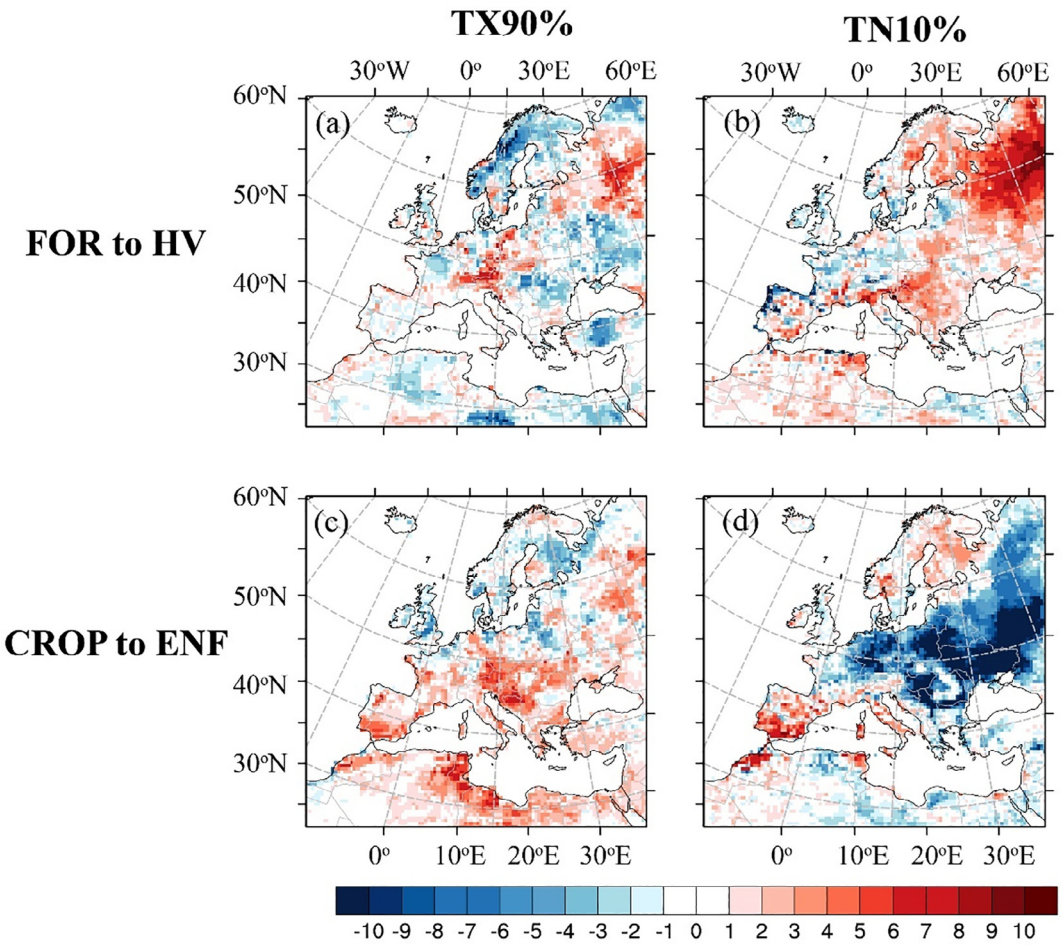

Fig. 2. Changes in number of days of temperature extremes measured in the different simulations relative to control simulation. Values show the average number of days with maximum daily temperature beyond the 90th percentile of the control run or minimum daily temperature below the 10th percentile of the control run.

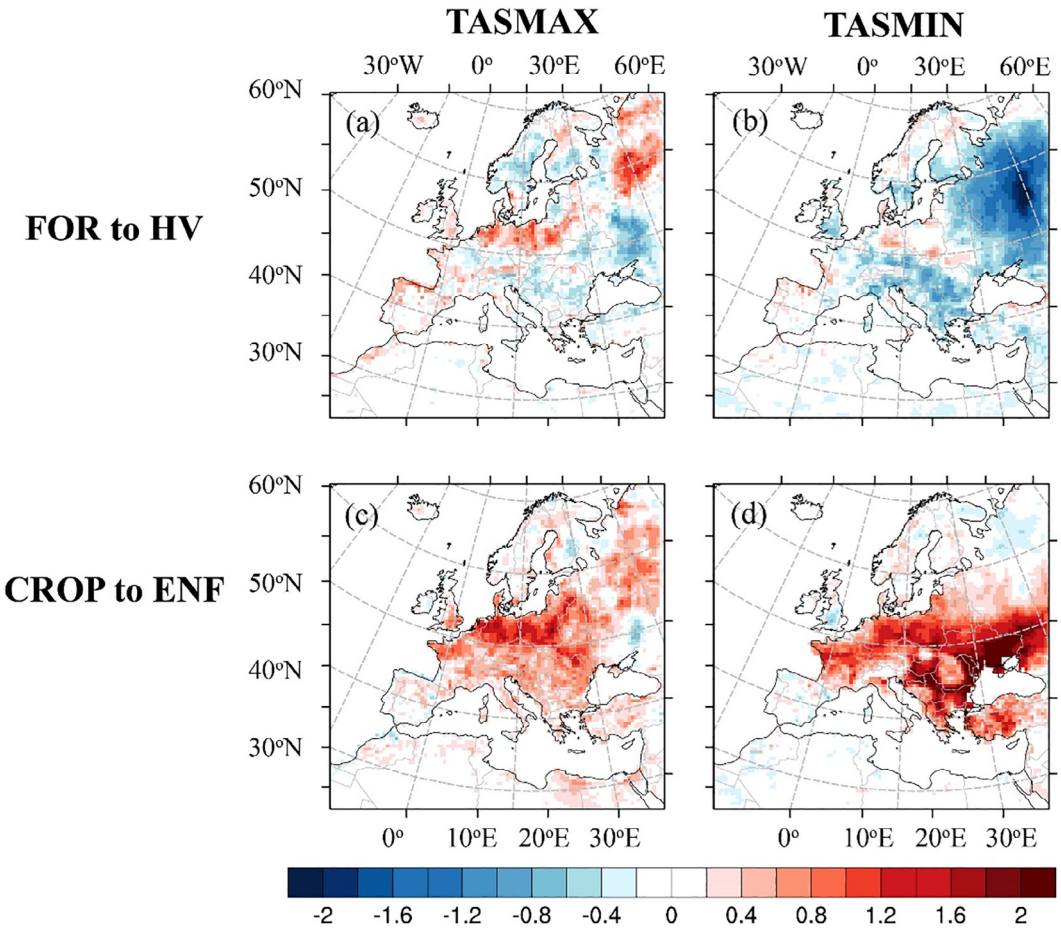

Fig. 3. Annual daily maximum (TASMAX) and minimum (TASMIN) temperature response to the simulated land cover changes in the deforestation (FOR to HV; a and b) and afforestation (CROP to ENF; c and d) simulations. Differences refer to 'simulation minus control'. Units: °C.

findings can be found in previous studies (Abiodun et al., 2013; Wang et al., 2014; Cherubini et al., 2018).

3.2. Changes in the intensity of the climate variables

There are changes in the intensity of TASMAX and TASMIN in the two simulations (Fig. 3). In the FOR to HV simulation, we find a slight lower TASMAX in most parts of the domain with significant higher TASMAX in Germany, Poland and northeast of the domain. However, the TASMIN consistently decreases over the whole domain, especially in the northeast, where massive deforestation happens. The maximum negative center is in the northeast part, where TASMIN is reduced up to −2 °C. In this simulation, the hot extreme gets hotter and the cold extreme gets colder, meaning that reduction in forest cover in Europe can further exacerbate the effects of climate change on humans and ecosystems.

In the CROP to ENF simulation, TASMAX and TASMIN show a similar positive response pattern. However, the warmest area differs, it is central Europe in TASMAX and east Europe in TASMIN. These results mean that afforestation increases both the hot and cold climate. This is mainly due to the type of tree considered for afforestation, because needle leaved forests have smaller evapotranspiration than grasses and broadleaved forest, especially during summer months. We further analyze the changes of empirical PDFs of the mean of TASMAX and TASMIN on regional and local scale for FOR to HV (Fig. 4) and CROP to ENF (Fig. 5) simulation. The simulated land cover changes alter the shapes and the ranges of the distributions. On the regional scale, the two peaks of TASMAX in the CTRL run tend to converge towards a single peak and higher values in the FOR to HV simulation (Fig. 4a), and are more smoothed in the CROP to ENF (Fig. 5a). The empirical PDFs for annual maximum of the TASMAX for both the deforestation and afforestation simulations also exhibit right longer tails than the CTRL run both on the regional and local scales. The explanation is a higher possibility of hot extremes occurrence when we cut down all the trees. On the other hand, the empirical PDFs of the TASMIN in the deforestation and afforestation simulations relative to the CTRL run behave differently. In the deforestation simulation, the PDF shifts to left at both regional and local level (Fig. 4b and d), meaning that the cold extremes become more severe. The opposite occurs in the afforestation simulation, where the severity of cold extremes is mitigated.

3.3. Changes in return level and return period

Return levels and return periods are commonly employed to characterize and quantify risks of extreme events. We compare the return levels and return periods of our deforestation and afforestation simulations with the CTRL simulation focusing on the hot extremes, i.e. the annual maximum of TASMAX.

We model the mean annual maximum of the TASMAX using the stationary GEV distribution since the likelihood-ratio test against the nonstationary model (with change in location parameter) returns a p-value much larger than the significant level of 0.05. This means that we cannot reject the null hypothesis with the stationary model. The application of the stationary GEV model in computing the return level and return period with the three simulations achieves good performance using quantile-quantile plots and the theoretical PDFs capture the empirical densities (not shown).

Both the deforestation and afforestation simulations significantly

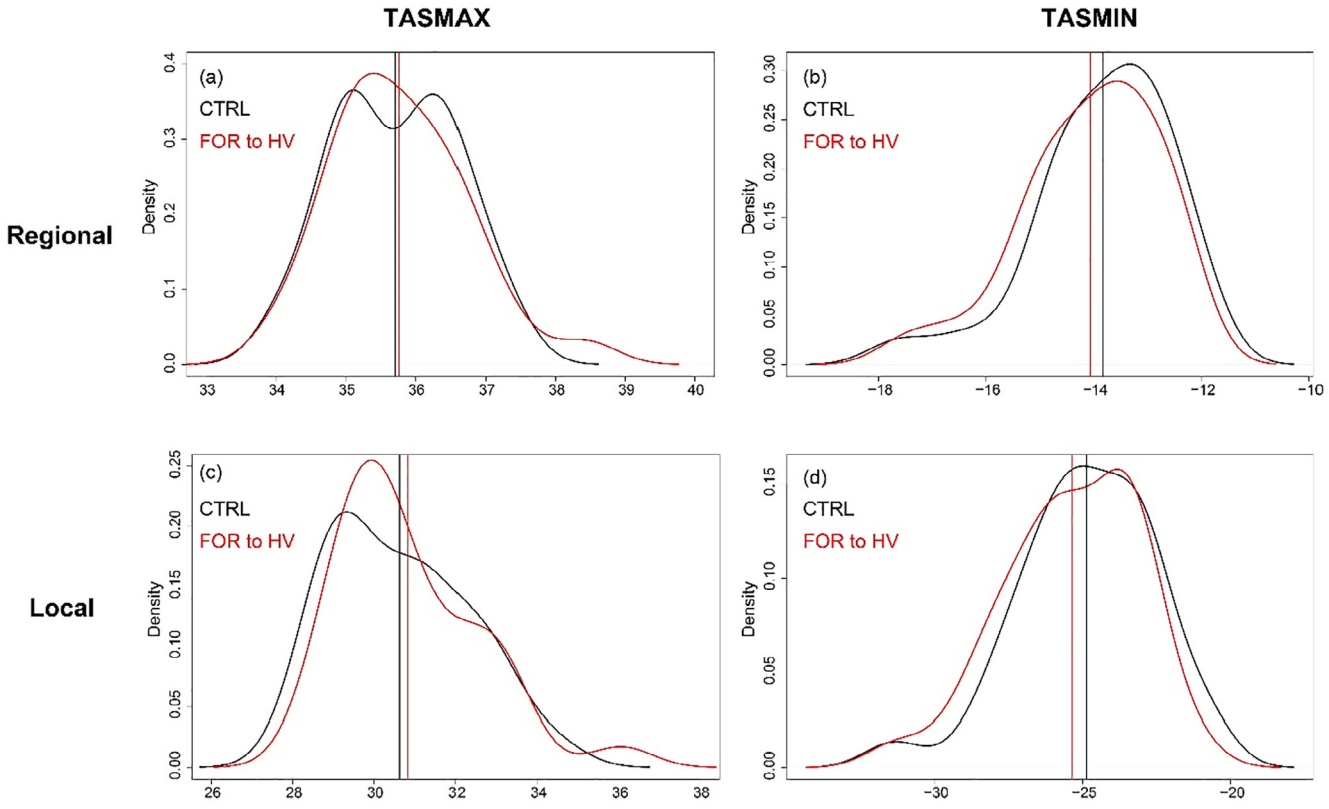

Fig. 4. Probability density distribution (PDF) of annual maximum of TASMAX (a and c) and annual minimum of TASMIN (b and d) on regional scale (a and b) and local scale (c and d) in CTRL (black lines) and FOR to HV simulation (red lines). The vertical solid line shows the mean value. Unit on x-axis: ˚C.

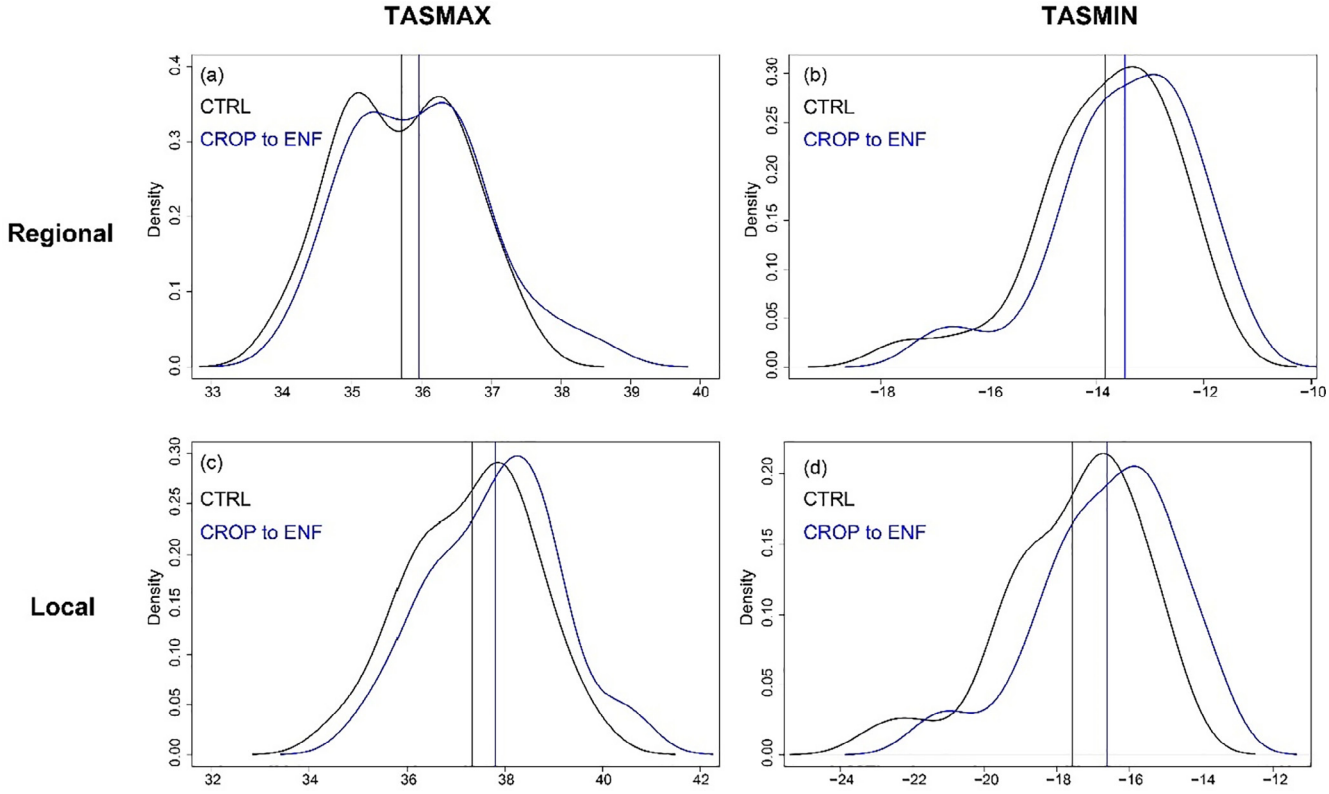

Fig. 5. Probability density distribution (PDF) of annual maximum TASMAX (a and c) and annual minimum TASMIN (b and d) on regional scale (a and b) and local scale (c and d) in CTRL (black lines) and CROP to ENF simulation (blue lines). The vertical solid line shows the mean value. Unit on x-axis: ˚C.

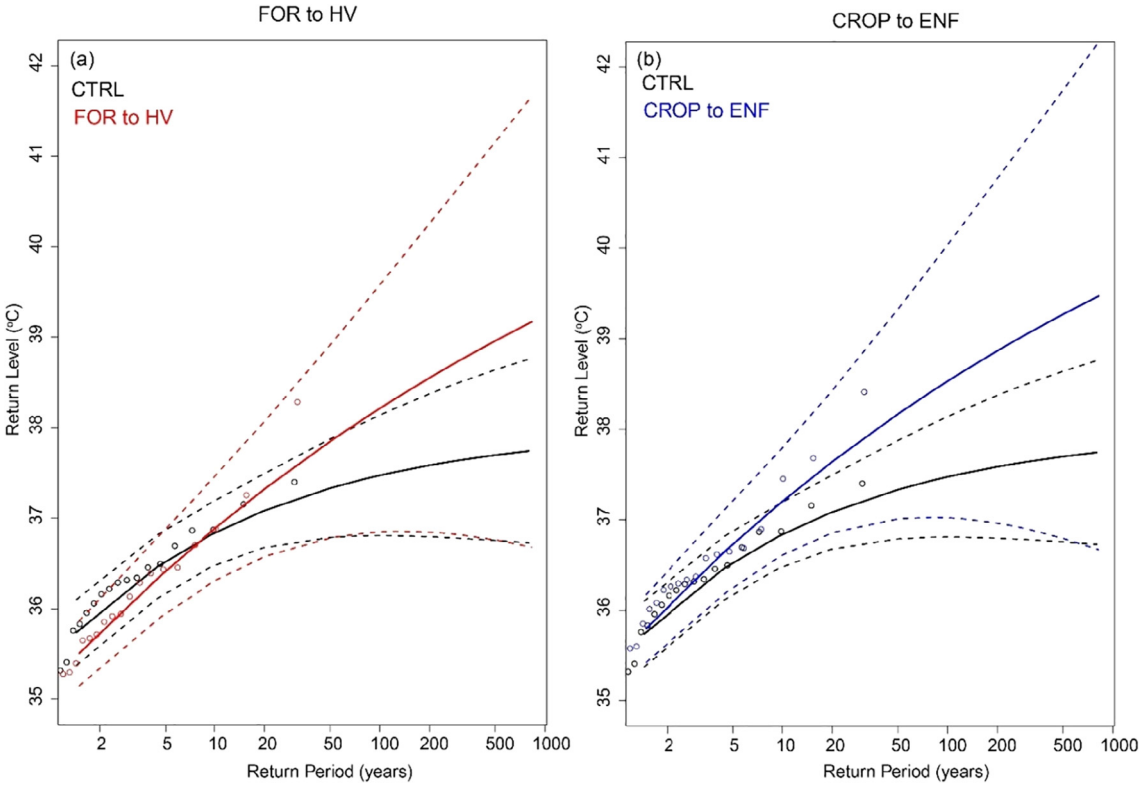

Fig. 6. Results of modelling the mean annual maximum temperature using the GEV distribution at a regional scale. Colored lines show the estimated return level in CTRL (black), in FOR to HV (red) and CROP to ENF (blue). The circles and the dashed-lines are the corresponding empirical estimates and 95% confidence intervals, respectively.

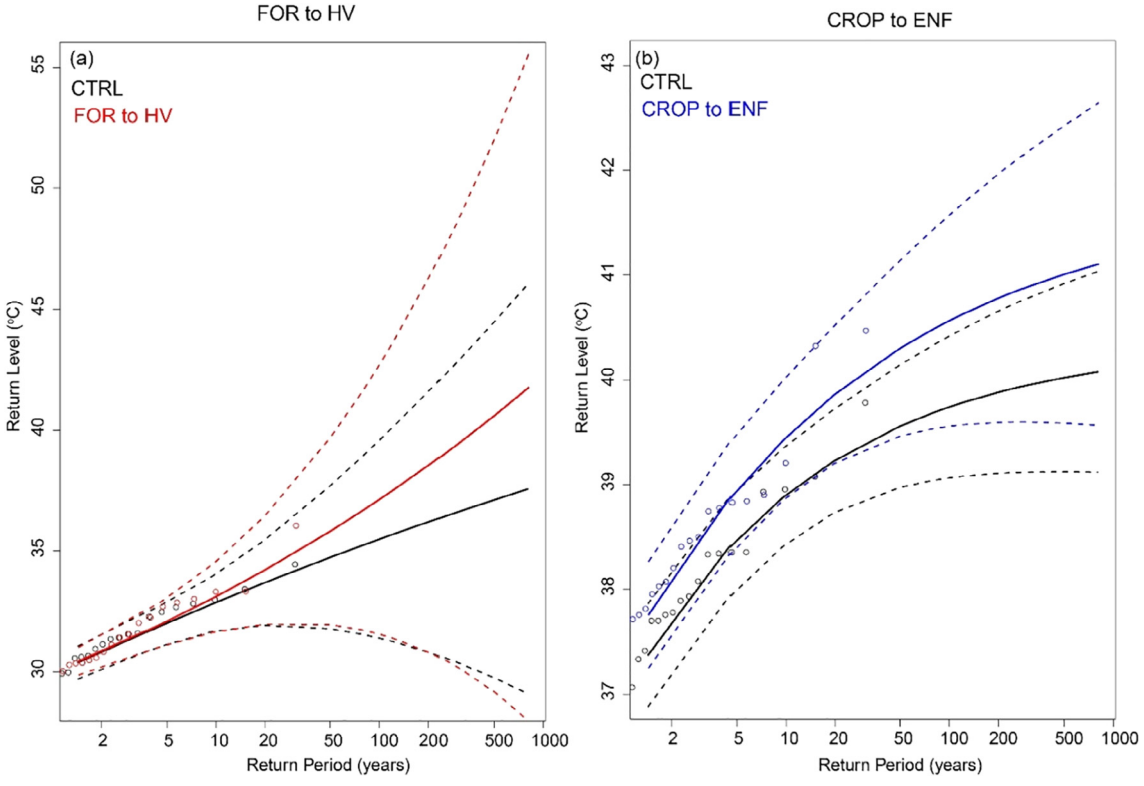

Fig. 7. Same as Fig. 6, but for grids effected by land cover change.

Table 3
Changes of m-year event 'simulation minus CTRL' in different simulations at different return levels. $m = \{20, 50, 100\}$.

	Regional					
	FOR to HV			CROP to ENF		
Return period (years)	20	50	100	20	50	100
Return level difference	0.41	0.69	0.92	0.62	0.91	1.14
	Local					
Return period (years)	20	50	100	20	50	100
Return level difference	0.53	1.09	1.67	0.67	0.77	0.85

change the return levels and return periods, especially for rare event, such as 50-year and 100-year events (Figs. 6 and 7). For instance, Fig. 6 shows that the return levels for return periods greater than 10 years increase with both deforestation and afforestation simulations and the upper bound of the return levels increases dramatically, which means that the risk of extreme heat is increasing (Fig. 6). The changes of return levels are more significant at local scale, though the changes follow the same pattern as at regional scale (Fig. 7). In the CTRL simulation, the upper bound of the 95% confidence interval of the 100-year return level is about 38 °C. However, this value increases to 39.8 °C and 42.7 °C with the FOR to HV simulation at the regional and local scale, respectively. In the CROP to ENF simulation, these values are increased to 40.1 °C and 41.6 °C, respectively.

Furthermore, the return levels for the m-years return period events, $m = 20, 50, 100$, increase in both the two simulations (Table 3). The change of return level for the 100-year return of the hot extreme increases up to 0.92 °C in deforestation simulation and 1.14 °C in afforestation simulation at the regional scale. At the local scale, it increases up to 1.67 °C in deforestation and 0.85 °C in afforestation simulation.

4. Discussion

Three simulations are conducted to investigate the changes in extreme events due to land cover changes. Changes in standard extreme indices and the intensity of the climate variables are reported, together with results on return level and return period. These results can be explained with the seasonality in the climate parameters, vegetation characteristics and associated surface properties. In winter, open land such as HV has higher albedo values than forested land and reflects more solar radiation back to the atmosphere, thereby reducing the amount of energy to be dissipated at the surface level. This results in an average cooling effect that affects extreme indices as well (Table 2). In winter, surface albedo dominates the local climate, especially in areas affected by seasonal snow cover (Betts et al., 2007; Anderson et al., 2011; Hu et al., 2018). Differences in evapotranspiration fluxes such as latent heat and sensible heat are minimal (Bathiany et al., 2010; Davin and de Noblet-Ducoudre, 2010; Li et al., 2015, 2016). On the other hand, the difference between albedo values is smaller in summer, and dominant role is evapotranspiration fluxes for summer climate (Galos et al., 2011; Zhang et al., 2014; Li et al., 2015). Forest areas have a higher partitioning of surface energy as latent heat instead of sensible heat than HV, which thus contributes to increase local temperature.

Our results are generally in line with other recent simulations that found significant changes in climate extremes after land cover change. There are still some differences in the sign of the response among the studies, mostly due to differences in the investigation approach, type of land cover parameterization and conversion, and climate model used. Some studies find that deforestation increases the hot extremes at the regional scale (Cherubini et al., 2018; Lejeune et al., 2018), while others draw an opposite conclusion (Pitman et al., 2012; Christidis et al., 2013). Afforestation increases evapotranspiration (Betts, 2011; Galos et al., 2011; Cherubini et al., 2018), and increase humidity. Our simulation shows that afforestation can lead to increases in the local hot extreme, in accordance to other studies (Wang et al., 2014; Cherubini et al., 2018), but in contrast to others (Galos et al., 2013). It is important to remind that our afforestation experiments consider needle leaved forests, which have lower evapotranspiration rates than broad-leaved forests, especially during summer. The consideration of the latter type of trees can lead to opposite results with respect to the effects on summer temperature (Naudts et al., 2016; Findell et al., 2017; Cherubini et al., 2018; Luyssaert et al., 2018; Tölle et al., 2018). Mitigation of cold extremes after afforestation is found in other articles as well (Abatan et al., 2018).

Our analysis uses a single model to perform the simulations. Results depend on model performance to various degrees in representing land surface processes, and inter-model comparison studies will be useful to compare different model outcomes, single out differences and investigate the dependencies of extremal events on different models with similar and different configurations and resolutions (Davin et al., 2016, 2019). This will help to increase the understanding of the climate system sensitivity in terms of extremes to land cover changes. More advanced simulations and model settings can also be used to assess the explicit impacts of biochemical and biophysical processes on the extreme events. Since the local climate conditions are sensitive to the exchanges of CO_2 between the atmosphere and vegetation (Friend et al., 2014; Sakaguchi et al., 2016), the dynamic response of the land cover change through phenology can reveal additional insights. Advanced statistical technics can also be used to quantify the statistical uncertainty of the severe climate events (Paciorek et al., 2018).

5. Conclusions

We employed the extreme value theory to investigate the impact of large-scale idealized LCCs on European extreme climate, using simulation outputs from a regional climate model (COSMO-CLM). We found that LCCs can modify not only the intensity and frequencies of the extremes but also the probability of the extreme events. The intensities of the hot extremes with both deforestation and afforestation increase together with higher frequencies. With deforestation, the cold extremes become more severe and their occurrence increases. On the other hand, afforestation mitigates the intensity and frequency of cold extremes. Furthermore, deforestation leads to a drier climate while afforestation produces a wetter climate. In general, the signal is stronger at the local scale than at the regional scale. LCCs significantly change the regional and local daily temperature extremes, and they shorten the return period of the extreme annual daily maximum.

Possible extensions of this work can consider the design of more realistic land cover changes associated to specific land management scenarios in Europe and quantify the associated impacts on extremes. Another possible direction is to quantify the influence on human society of extreme climate, thereby directly coupling climate modelling with a society dimension (Patz et al., 2005; Mitchell et al., 2016; Mora et al., 2017; Paciorek et al., 2018). Detection and attribution is also a useful pathway to study and attribute the trends of different forces (Trenberth et al., 2015; Easterling et al., 2016; Stott et al., 2016; Lu et al., 2018). Since extreme events have large impact on the ecosystem and human society, changes in such events due to land cover management need to be taken into consideration by the local or regional authorities and ideally factored in decision processes. The ultimate goal is to refine land management strategies in light of climate change mitigation and adaptation.

Acknowledgements

This work is supported by the Norwegian Research Council (grants nr. 244074 and 254966). COSMO-CLM is the community model of the German regional climate research jointly further developed by the CLM-Community (www.clm-community.eu/). Simulations were performed on resources provided by UNINETT Sigma2—the National

Infrastructure for High Performance Computing and Data Storage in Norway. We acknowledge two anonymous reviewers for their useful inputs to the manuscript.

References

Abatan, A.A., Osayomi, T., Akande, S.O., Abiodun, B.J., Gutowski, W.J., 2018. Trends in mean and extreme temperatures over Ibadan, Southwest Nigeria. Theor. Appl. Climatol. 131, 1261–1272.

Abiodun, B.J., Salami, A.T., Matthew, O.J., Odedokun, S., 2013. Potential impacts of afforestation on climate change and extreme events in Nigeria. Clim. Dyn. 41, 277–293.

AghaKouchak, A., Easterling, D., Hsu, K., Schubert, S., Sorooshian, S., 2012. Extremes in a Changing Climate: Detection, Analysis and Uncertainty. Springer Science & Business Media, Berlin.

Aldieri, L., Vinci, C.P., 2018. Green economy and sustainable development: the economic impact of innovation on employment. Sustainability 10, 3541.

Alexander, L.V., Zhang, X., Peterson, T.C., Caesar, J., Gleason, B., Tank, A.M.G.K., Haylock, M., Collins, D., Trewin, B., Rahimzadeh, F., Tagipour, A., Kumar, K.R., Revadekar, J., Griffiths, G., Vincent, L., Stephenson, D.B., Burn, J., Aguilar, E., Brunet, M., Taylor, M., New, M., Zhai, P., Rusticucci, M., Vazquez-Aguirre, J.L., 2006. Global observed changes in daily climate extremes of temperature and precipitation. J. Geophys. Res. 111, D05109.

Ament, F., Simmer, C., 2006. Improved representation of land-surface heterogeneity in a non-hydrostatic numerical weather prediction model. Bound.-Layer Meteorol. 121, 153–174.

Anderson, R.G., Canadell, J.G., Randerson, J.T., Jackson, R.B., Hungate, B.A., Baldocchi, D.D., Ban-Weiss, G.A., Bonan, G.B., Caldeira, K., Cao, L., 2011. Biophysical considerations in forestry for climate protection. Front. Ecol. Environ. 9, 174–182.

Arakawa, A., Lamb, V.R., 1981. A potential enstrophy and energy conserving scheme for the shallow-water equations. Mon. Weather Rev. 109, 18–36.

Arora, V.K., Peng, Y., Kurz, W.A., Fyfe, J.C., Hawkins, B., Werner, A.T., 2016. Potential near-future carbon uptake overcomes losses from a large insect outbreak in British Columbia, Canada. Geophys. Res. Lett. 43, 2590–2598.

Astrom, D.O., Forsberg, B., Ebi, K.L., Rocklov, J., 2013. Attributing mortality from extreme temperatures to climate change in Stockholm, Sweden. Nat. Clim. Change 3, 1050–1054.

Bala, G., Caldeira, K., Wickett, M., Phillips, T.J., Lobell, D.B., Delire, C., Mirin, A., 2007. Combined climate and carbon-cycle effects of large-scale deforestation. Proc. Natl. Acad. Sci. U.S.A. 104, 6550–6555.

Bathiany, S., Claussen, M., Brovkin, V., Raddatz, T., Gayler, V., 2010. Combined biogeophysical and biogeochemical effects of large-scale forest cover changes in the MPI earth system model. Biogeosciences 7, 1383–1399.

Beirlant, J., Goegebeur, Y., Segers, J., Teugels, J.L., 2006. Statistics of Extremes: Theory and Applications. John Wiley & Sons.

Betts, R.A., 2011. CLIMATE SCIENCE Afforestation cools more or less. Nat. Geosci. 4, 504–505.

Betts, R.A., Falloon, P.D., Goldewijk, K.K., Ramankutty, N., 2007. Biogeophysical effects of land use on climate: model simulations of radiative forcing and large-scale temperature change. Agric. For. Meteorol. 142, 216–233.

Cheng, L.Y., AghaKouchak, A., Gilleland, E., Katz, R.W., 2014. Non-stationary extreme value analysis in a changing climate. Clim. Change 127, 353–369.

Cherubini, F., Fuglestvedt, J., Gasser, T., Reisinger, A., Cavalett, O., Huijbregts, M.A.J., Johansson, D.J.A., Jorgensen, S.V., Raugei, M., Schivley, G., Stromman, A.H., Tanaka, K., Levasseur, A., 2016. Bridging the gap between impact assessment methods and climate science. Environ. Sci. Policy 64, 129–140.

Cherubini, F., Huang, B., Hu, X.P., Tolle, M.H., Stromman, A.H., 2018. Quantifying the climate response to extreme land cover changes in Europe with a regional model. Environ. Res. Lett. 13, 074002.

Christidis, N., Stott, P.A., Hegerl, G.C., Betts, R.A., 2013. The role of land use change in the recent warming of daily extreme temperatures. Geophys. Res. Lett. 40, 589–594.

Coles, S., Bawa, J., Trenner, L., Dorazio, P., 2001. An Introduction to Statistical Modeling of Extreme Values. Springer, Berlin.

Cooley, D., 2013. Return periods and return levels under climate change. In: Extremes in a Changing Climate. Springer, Berlin, pp. 97–114.

Davin, E.L., de Noblet-Ducoudre, N., 2010. Climatic impact of global-scale deforestation: radiative versus nonradiative processes. J. Clim. 23, 97–112.

Davin, E.L., Seneviratne, S.I., Ciais, P., Olioso, A., Wang, T., 2014. Preferential cooling of hot extremes from cropland albedo management. Proc. Natl. Acad. Sci. U.S.A. 111, 9757–9761.

Davin, E.L., Maisonnave, E., Seneviratne, S.I., 2016. Is land surface processes representation a possible weak link in current Regional Climate Models? Environ. Res. Lett. 11.

Davin, E.L., Rechid, D., Breil, M., Cardoso, R.M., Coppola, E., Hoffmann, P., Jach, L.L., Katragkou, E., de Noblet-Ducoudré, N., Radtke, K., Raffa, M., Soares, P.M.M., Sofiadis, G., Strada, S., Strandberg, G., Tölle, M.H., Warrach-Sagi, K., Wulfmeyer, V., 2019. Biogeophysical impacts of forestation in Europe: first results from the LUCAS Regional Climate Model intercomparison. Earth Syst. Dynam. Discuss. 2019, 1–31.

Dee, D.P., Uppala, S.M., Simmons, A.J., Berrisford, P., Poli, P., Kobayashi, S., Andrae, U., Balmaseda, M.A., Balsamo, G., Bauer, P., Bechtold, P., Beljaars, A.C.M., van de Berg, L., Bidlot, J., Bormann, N., Delsol, C., Dragani, R., Fuentes, M., Geer, A.J., Haimberger, L., Healy, S.B., Hersbach, H., Holm, E.V., Isaksen, L., Kallberg, P., Kohler, M., Matricardi, M., McNally, A.P., Monge-Sanz, B.M., Morcrette, J.J., Park, B.K., Peubey, C., de Rosnay, P., Tavolato, C., Thepaut, J.N., Vitart, F., 2011. The ERA-Interim reanalysis: configuration and performance of the data assimilation system. Q. J. R. Meteorolog. Soc. 137, 553–597.

Doms, G., Schättler, U., 2002. A Description of the Nonhydrostatic Regional Model LM. Part I: Dynamics and Numerics. Deutscher Wetterdienst, Offenbach.

Easterling, D.R., Meehl, G.A., Parmesan, C., Changnon, S.A., Karl, T.R., Mearns, L.O., 2000. Climate extremes: observations, modeling, and impacts. Science 289, 2068–2074.

Easterling, D.R., Kunkel, K.E., Wehner, M.E., Sun, L.Q., 2016. Detection and attribution of climate extremes in the observed record. Weather Clim. Extremes 11, 17–27.

Findell, K.L., Pitman, A.J., England, M.H., Pegion, P.J., 2009. Regional and global impacts of land cover change and sea surface temperature anomalies. J. Clim. 22, 3248–3269.

Findell, K.L., Berg, A., Gentine, P., Krasting, J.P., Lintner, B.R., Malyshev, S., Santanello Jr., J.A., Shevliakova, E., 2017. The impact of anthropogenic land use and land cover change on regional climate extremes. Nat. Commun. 8, 989.

Fischer, E.M., Knutti, R., 2015. Anthropogenic contribution to global occurrence of heavy-precipitation and high-temperature extremes. Nat. Clim. Change 5, 560–564.

Frich, P., Alexander, L.V., Della-Marta, P., Gleason, B., Haylock, M., Tank, A.M.G.K., Peterson, T., 2002. Observed coherent changes in climatic extremes during the second half of the twentieth century. Clim. Res. 19, 193–212.

Friend, A.D., Lucht, W., Rademacher, T.T., Keribin, R., Betts, R., Cadule, P., Ciais, P., Clark, D.B., Dankers, R., Falloon, P.D., Ito, A., Kahana, R., Kleidon, A., Lomas, M.R., Nishina, K., Ostberg, S., Pavlick, R., Peylin, P., Schaphoff, S., Vuichard, N., Warszawski, L., Wiltshire, A., Woodward, F.I., 2014. Carbon residence time dominates uncertainty in terrestrial vegetation responses to future climate and atmospheric CO2. Proc. Natl. Acad. Sci. U.S.A. 111, 3280–3285.

Galos, B., Matyas, C., Jacob, D., 2011. Regional characteristics of climate change altering effects of afforestation. Environ. Res. Lett. 6, 044010.

Galos, B., Hagemann, S., Hansler, A., Kindermann, G., Rechid, D., Sieck, K., Teichmann, C., Jacob, D., 2013. Case study for the assessment of the biogeophysical effects of a potential afforestation in Europe. Carbon Balance Manage. 8, 3.

Gilleland, E., Katz, R.W., 2016. extRemes 2.0: an extreme value analysis package in R. J. Stat. Softw. 72, 1–39.

Gilleland, E., Ribatet, M., Stephenson, A.G., 2013. A software review for extreme value analysis. Extremes 16, 103–119.

Glc, B.A., 2005. a new approach to global land covermapping from Earth observation data/AS Belward. Int. J. Remote Sens. 26, 1959–1977.

Gomes, M.I., Guillou, A., 2015. Extreme value theory and statistics of univariate extremes: a review. Int. Statistical Rev. 83, 263–292.

Hájek, P., Stejskal, J., 2018. R&D cooperation and knowledge spillover effects for sustainable business innovation in the chemical industry. Sustainability 10, 1064.

Hegerl, G.C., Zwiers, F.W., Braconnot, P., Gillett, N.P., Luo, Y., Marengo Orsini, J., Nicholls, N., Penner, J.E., Stott, P.A., 2007. Understanding and attributing climate change. In: IPCC, 2007: Climate Change 2007: The Physical Science Basis. Contribution of Working Group I to the Fourth Assessment Report of the Intergovernmental Panel on Climate Change. Cambridge University Press, Cambridge, UK.

Hu, X.P., Cherubini, F., Vezhapparambu, S., Stromman, A.H., 2018. From remotely-sensed data of Norwegian boreal forests to fast and flexible models for estimating surface albedo. J. Adv. Model. Earth Syst. 10, 2495–2513.

Katz, R.W., 2013. Extremes in a changing climate. In: Statistical Methods for Nonstationary Extremes. Springer, Berlin, pp. 15–37.

Katz, R.W., Parlange, M.B., Naveau, P., 2002. Statistics of extremes in hydrology. Adv. Water Resour. 25, 1287–1304.

Klein Tank, A., Können, G.P., 2003. Trends in indices of daily temperature and precipitation extremes in Europe. J. Climate 16, 3665–3680.

Kotlarski, S., Keuler, K., Christensen, O.B., Colette, A., Deque, M., Gobiet, A., Goergen, K., Jacob, D., Luthi, D., van Meijgaard, E., Nikulin, G., Schar, C., Teichmann, C., Vautard, R., Warrach-Sagi, K., Wulfmeyer, V., 2014. Regional climate modeling on European scales: a joint standard evaluation of the EURO-CORDEX RCM ensemble. Geosci. Model Dev. 7, 1297–1333.

Lejeune, Q., Davin, E.L., Gudmundsson, L., Winckler, J., Seneviratne, S.I., 2018. Historical deforestation locally increased the intensity of hot days in northern mid-latitudes. Nature Clim. Change 8, 386–390.

Li, Y., Zhao, M., Motesharrei, S., Mu, Q., Kalnay, E., Li, S., 2015. Local cooling and warming effects of forests based on satellite observations. Nat. Commun. 6, 6603.

Li, Y., De Noblet-Ducoudre, N., Davin, E.L., Motesharrei, S., Zeng, N., Li, S.C., Kalnay, E., 2016. The role of spatial scale and background climate in the latitudinal temperature response to deforestation. Earth Syst. Dyn. 7, 167–181.

Lu, C.H., Sun, Y., Zhang, X.B., 2018. Multimodel detection and attribution of changes in warm and cold spell durations. Environ. Res. Lett. 13.

Luyssaert, S., Marie, G., Valade, A., Chen, Y.Y., Njakou Djomo, S., Ryder, J., Otto, J., Naudts, K., Lanso, A.S., Ghattas, J., McGrath, M.J., 2018. Trade-offs in using European forests to meet climate objectives. Nature 562, 259–262.

Mellor, G.L., Yamada, T., 1982. Development of a turbulence closure-model for geophysical fluid problems. Rev. Geophys. 20, 851–875.

Mitchell, D., Heaviside, C., Vardoulakis, S., Huntingford, C., Masato, G., Guillod, B.P., Frumhoff, P., Bowery, A., Wallom, D., Allen, M., 2016. Attributing human mortality during extreme heat waves to anthropogenic climate change. Environ. Res. Lett. 11, 074006.

Mora, C., Dousset, B., Caldwell, I.R., Powell, F.E., Geronimo, R.C., Bielecki, C.R., Counsell, C.W., Dietrich, B.S., Johnston, E.T., Louis, L.V., Lucas, M.P., McKenzie, M.M., Shea, A.G., Tseng, H., Giambelluca, T., Leon, L.R., Hawkins, E., Trauernicht, C., 2017. Global risk of deadly heat. Nature Clim. Change 7, 501–506.

Naudts, K., Chen, Y., McGrath, M.J., Ryder, J., Valade, A., Otto, J., Luyssaert, S., 2016. Europe's forest management did not mitigate climate warming. Science 351, 597–600.

Naveau, P., Nogaj, M., Ammann, C., Yiou, P., Cooley, D., Jomelli, V., 2005. Statistical methods for the analysis of climate extremes. C.R. Geosci. 337, 1013–1022.
Paciorek, C.J., Stone, D.A., Wehner, M.F., 2018. Quantifying statistical uncertainty in the attribution of human influence on severe weather. Weather Clim. Extremes 20, 69–80.
Patz, J.A., Campbell-Lendrum, D., Holloway, T., Foley, J.A., 2005. Impact of regional climate change on human health. Nature 438, 310–317.
Peterson, T., Anderson, D., Cohen, S., Cortez-Vázquez, M., Murnane, R., Parmesan, C., Phillips, D., Pulwarty, R., Stone, J., 2008. In: Why weather and climate extremes matter. Weather and Climate Extremes in a Changing Climate. Regions of Focus: North America. US Pacific Islands, Hawaii, Caribbean, pp. 11–33.
Peterson, T., Folland, C., Gruza, G., Hogg, W., Mokssit, A., Plummer, N., 2001. Report on the Activities of the Working Group on Climate Change Detection and Related Rapporteurs. World Meteorological Organization Geneva.
Pirard, P., Vandentorren, S., Pascal, M., Laaidi, K., Le Tertre, A., Cassadou, S., Ledrans, M., 2005. Summary of the mortality impact assessment of the 2003 heat wave in France. Euro Surveill 10, 153–156.
Pitman, A.J., de Noblet-Ducoudre, N., Avila, F.B., Alexander, L.V., Boisier, J.P., Brovkin, V., Delire, C., Cruz, F., Donat, M.G., Gayler, V., van den Hurk, B., Reick, C., Voldoire, A., 2012. Effects of land cover change on temperature and rainfall extremes in multi-model ensemble simulations. Earth Syst. Dyn. 3, 213–231.
Reiss, R.-D., Thomas, M., Reiss, R., 2007. Statistical Analysis of Extreme Values. Springer, Berlin.
Ritter, B., Geleyn, J.F., 1992. A comprehensive radiation scheme for numerical weather prediction models with potential applications in climate simulations. Mon. Weather Rev. 120, 303–325.
Rockel, B., Will, A., Hense, A., 2008. The regional climate model COSMO-CLM(CCLM). Meteorologische Zeitschrift 17, 347–348.
Sakaguchi, K., Zeng, X., Leung, L.R., Shao, P., 2016. Influence of dynamic vegetation on carbon-nitrogen cycle feedback in the Community Land Model (CLM4). Environ. Res. Lett. 11, 124029.
Schär, C., Leuenberger, D., Fuhrer, O., Luthi, D., Girard, C., 2002. A new terrain-following vertical coordinate formulation for atmospheric prediction models. Mon. Weather Rev. 130, 2459–2480.
Schrodin, R., Heise, E., 2001. The multi-layer version of the DWD soil model TERRA-LM. Consortium for Small-Scale Modelling (COSMO). Tech. Rep. 2, 16.
Seidl, R., Schelhaas, M.-J., Rammer, W., Verkerk, P.J., 2014. Increasing forest disturbances in Europe and their impact on carbon storage. Nat. Clim. Change 4, 806–810.
Seneviratne, S.I., Corti, T., Davin, E.L., Hirschi, M., Jaeger, E.B., Lehner, I., Orlowsky, B., Teuling, A.J., 2010. Investigating soil moisture-climate interactions in a changing climate: a review. Earth Sci. Rev. 99, 125–161.
Seneviratne, S.I., Easterling, D., Goodess, C.M., Kanae, S., Kossin, J., Luo, Y., Marengo, J., McInnes, K., Rahimi, M., Reichstein, M., 2012. Changes in Climate Extremes and their Impacts on the Natural Physical Environment. In: Managing the Risks of Extreme Events and Disasters to Advance Climate Change Adaptation: Special Report of the Intergovernmental Panel on Climate Change. Cambridge University Press, Cambridge, pp. 109–230.
Sheikh, M., Manzoor, N., Ashraf, J., Adnan, M., Collins, D., Hameed, S., Manton, M., Ahmed, A., Baidya, S., Borgaonkar, H.P., 2015. Trends in extreme daily rainfall and temperature indices over South Asia. Int. J. Climatol. 35, 1625–1637.
Stefanon, M., Drobinski, P., D'Andrea, F., Lebeaupin-Brossier, C., Bastin, S., 2014. Soil moisture-temperature feedbacks at meso-scale during summer heat waves over Western Europe. Clim. Dyn. 42, 1309–1324.
Stott, P.A., Christidis, N., Otto, F.E., Sun, Y., Vanderlinden, J.P., van Oldenborgh, G.J., Vautard, R., von Storch, H., Walton, P., Yiou, P., Zwiers, F.W., 2016. Attribution of extreme weather and climate-related events. WIREs Clim. Change 7, 23–41.
Tank, A.M.G.K., Zwiers, F.W., Zhang, X., 2009. Guidelines on analysis of extremes in a changing climate in support of informed decisions for adaptation. Climate data and monitoring WCDMP-No. 72, WMO-TD No. 1500 2009, 56.
Tiedtke, M., 1989. A comprehensive mass flux scheme for cumulus parameterization in large-scale models. Mon. Weather Rev. 117, 1779–1800.
Tölle, M.H., Gutjahr, O., Busch, G., Thiele, J.C., 2014. Increasing bioenergy production on arable land: does the regional and local climate respond? Germany as a case study. J. Geophys. Res.: Atmospheres 119, 2711–2724.
Tölle, M.H., Engler, S., Panitz, H.J., 2017. Impact of abrupt land cover changes by tropical deforestation on Southeast Asian climate and agriculture. J. Clim. 30, 2587–2600.
Tölle, M.H., Panitz, H.-J., Breil, M., Radtke, K., 2018. Sensitivity of European temperature to albedo parameterization in the regional climate model COSMO-CLM linked to extreme land use changes. Front. Environ. Sci. 6, 123.
Trenberth, K.E., Fasullo, J.T., Shepherd, T.G., 2015. Attribution of climate extreme events. Nat. Clim. Change 5, 725–730.
Vincent, L.A., Mekis, E.J.A.-O., 2006. Changes in daily and extreme temperature and precipitation indices for Canada over the twentieth century. Atmosphere-Ocean 44, 177–193.
Wang, Y., Yan, X.D., Wang, Z.M., 2014. The biogeophysical effects of extreme afforestation in modeling future climate. Theor. Appl. Climatol. 118, 511–521.
Wicker, L.J., Skamarock, W.C., 2002. Time-splitting methods for elastic models using forward time schemes. Mon. Weather Rev. 130, 2088–2097.
Zhang, X.B., Alexander, L., Hegerl, G.C., Jones, P., Tank, A.K., Peterson, T.C., Trewin, B., Zwiers, F.W., 2011. Indices for monitoring changes in extremes based on daily temperature and precipitation data. Wiley Interdiscip. Rev.-Climate Change 2, 851–870.
Zhang, M., Lee, X.H., Yu, G.R., Han, S.J., Wang, H.M., Yan, J.H., Zhang, Y.P., Li, Y.D., Ohta, T., Hirano, T., Kim, J., Yoshifuji, N., Wang, W., 2014. Response of surface air temperature to small-scale land clearing across latitudes. Environ. Res. Lett. 9, 034002.
Zhang, X., Zwiers, F.W., 2013. Statistical indices for the diagnosing and detecting changes in extremes. In: Extremes in a Changing Climate. Springer, Berlin.